

pubs.acs.org/JPCC Article

Enhanced Plasma Generation from Metal Nanostructures via Photoexcited Hot Electrons

Bofan Zhao, Indu Aravind, Sisi Yang, Yu Wang, Ruoxi Li, Boxin Zhang, Yi Wang, Jahan M. Dawlaty, and Stephen B. Cronin*



Cite This: https://doi.org/10.1021/acs.jpcc.1c00765



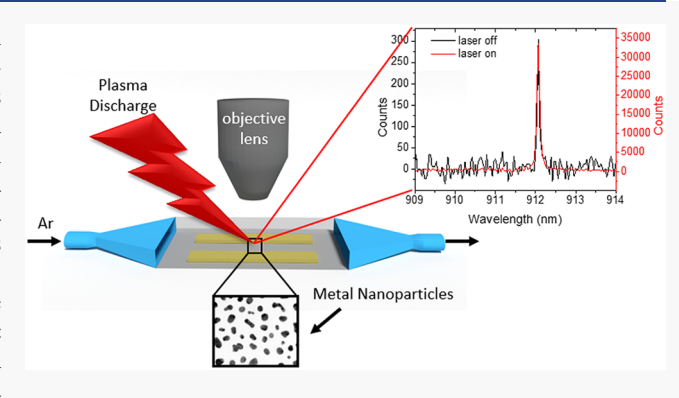
ACCESS

III Metrics & More

Article Recommendations

s Supporting Information

ABSTRACT: We report hot electron-enhanced plasma generation by irradiating metal nanostructures with laser light. Here, a high-voltage nanosecond pulse is discharged across two electrodes interspersed with metal nanoparticles (e.g., Au and Pt) both with and without laser excitation. With laser excitation (532 nm in wavelength), we observe a 200-fold increase in the plasma emission intensity (i.e., plasma density) and a lower threshold for the onset of plasma discharge (i.e., lower voltage). This enhancement of plasma emission/discharge occurs for two reasons. First, the hot electrons photoexcited in these metals lower the effective work function that needs to be overcome for thermionic emission, thus initiating the plasma. Second, the metal nanostructures minimize the average distance the photoexcited



carriers (i.e., hot electrons) have to travel to reach the surface. As such, the photoexcited hot carriers within the metal nanostructures can easily reach the surface before relaxing back to equilibrium. While these metal nanostructures have been shown to be strongly plasmonic (e.g., Au nanoparticles), we believe that the plasmon resonance does not play an important role in this plasma emission process. Plasma emission under 633 and 785 nm laser wavelength irradiation was also tested, but no enhancement in plasma emission was observed. We attribute this to the low photon energy (i.e., 1.9 eV), which lies below the threshold for interband transitions in Au and Pt.

■ INTRODUCTION

Hot electrons photoexcited in metals have been extensively discussed over the past decade as a novel mechanism for driving different chemical reactions 1-4 as well as solid-state electronic devices.⁵⁻⁸ For example, Guo et al. used Au/Pd superstructures to improve hot electron utilization and further enhance catalytical performance in the activation of molecular oxygen as well as C-C coupling reactions.9 Hot electrondoped MoS2 was also shown to provide a better catalytical surface compared with its undoped counterpart in driving hydrogen evolution reactions. 10 In solid-state devices, tunneling of hot electrons was utilized in hot electron transistors (HETs), and HETs fabricated with semiconductor materials with bipolar¹¹ and unipolar¹² designs were reported. 2D materials, such as graphene, was also used in HETs, and later works demonstrated both in-plane and vertical HET structures with graphene. High-performance IR detectors were also realized by using hot electron generation in Schottky junctionbased semiconductor devices . 15,16 In addition, plasmon resonant absorption was also utilized and plasmonic hot electron IR detectors were fabricated with a detectivity of 4.38 \times 10¹¹ cm Hz^{1/2}/W.^{15,17} As far back as 1961, electron emission from discontinuous metal ultrathin films was reported to

explain the electron conduction behavior of metal island films and its deviation from Ohm's law. 18 This deviation was first considered to be the result of field emission of electrons from the small metal islands by Dittmer in 1972.¹⁹ However, it was revealed that hot electrons, generated in nanoparticles (NPs) within the length scale of the hot electron mean free path, play a predominant role in this process.²⁰⁻²³ Previous work by Zhao et al. reported that plasma discharge across metal NP substrates can be enhanced up to 1000-fold as a result of locally enhanced electrostatic fields at the surface of these NPs in the absence of laser light, and this work indicated the importance of electron emission from metal NPs in the plasma generation mechanism.²⁴ Previous work using a similar approach also demonstrated up to 50-fold enhancement in C₂ radicals in the plasma-driven upconversion of methane. While these previous studies indicate the great promise for

Received: January 27, 2021 Revised: March 10, 2021



discharging nanosecond high-voltage pulses across Au nanoparticles (AuNPs), no previous measurements have been done using laser excitation in conjunction.²⁵

Lasers have been used to generate plasma for several decades in a process referred to as laser-induced plasma (LIP). Here, high-energy laser pulses deliver a significant amount of energy onto the surface of target materials, leading to vaporization, excitation, and ionization of materials on these surfaces. 26-2 As a result, materials on the surface can be excited into a plasma state, and this process has been used in material characterization (e.g., laser-induced breakdown spectroscopy) and pulsed laser deposition. 29-32 Essentially, LIP involves exciting solid materials into the plasma phase, which is quite distinct from our work presented here, in which gaseous species are excited into the plasma phase using a combination of applied electrical and optical fields.

METHOD

Here, a cold (i.e., nonthermal) plasma is generated from nanosecond, high-voltage pulses (SSPG-20X, Transient Plasma Systems, Inc.). Figure 1a shows a typical waveform of the pulse characteristics, which exhibit a 5-10 ns rise time. These nanosecond high-voltage pulse discharges create a relatively cold (nonthermal) plasma, which protects the integrity of NPs. With these high-voltage pulses, the electric field collapses

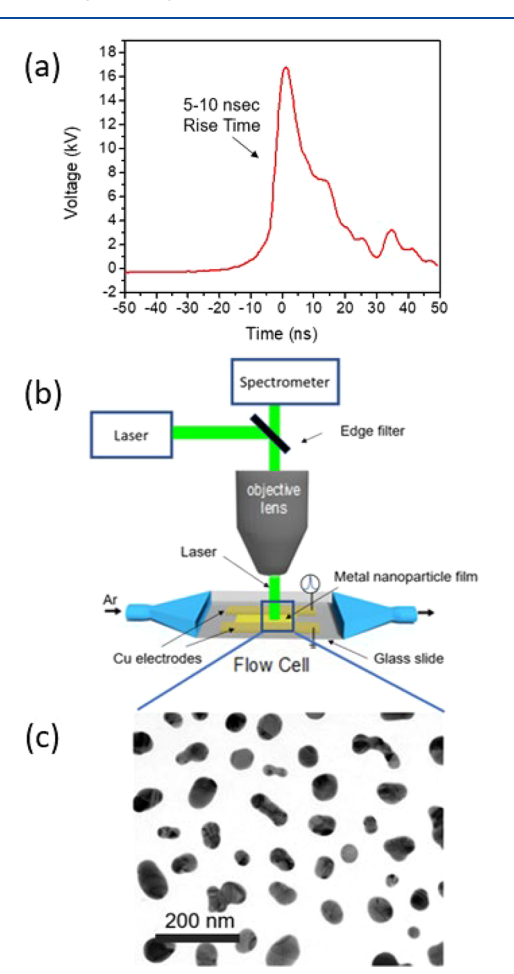


Figure 1. (a) Typical output waveform from the high-voltage nanosecond pulse generator, (b) a schematic diagram of the experimental setup for observation of optical emission, and (c) HRTEM image of the NP morphology deposited on glass slides.

before a significant amount of current flows in the system, and plasma ignition occurs without producing a substantial amount of heat. In order to evaluate the enhancement produced by laser-induced hot electrons, we monitor the emission spectra of argon plasma discharge (912.3 nm line) at different peak pulse voltages both with and without laser irradiation. The 912.3 nm line corresponds to an optical transition in neutral argon from the 4p state to the 4s state.³³ Argon emission spectra are collected from a region between two parallel copper electrodes, which are made by depositing Cu tape on a standard glass slide, interspersed with metal NPs in a flowing Ar environment, as illustrated in Figure 1b,c. We flow Ar at a rate of 100 sccm, and the plasma discharge is created by high-voltage pulses at a repetition rate of 1 kHz repetition rate. The emission spectra were collected in a Renishaw inVia micro-Raman spectrometer, and the objective lens used in this work was an Olympus LUCPlanFLN 40× cover-glass corrected lens. Photographs of our experimental setup are presented in Figure S1 of the Supporting Information. Figure 1c shows a typical highresolution transmission electron microscope (HRTEM) image of the metal NPs used in this work, deposited via electron beam evaporation with a nominal thickness of 5-10 nm.³⁴ As shown in Figure 1c, this thickness is not enough to form a continuous metal thin film and, instead, creates thin island-like structures or "NPs."

RESULTS AND DISCUSSION

Figure 2 shows the plasma emission intensity plotted as a function of peak pulse voltage for an electrode gap containing platinum NPs. This plot shows two datasets, one with the laser on and the other with the laser off, showing up to 200-fold increase in the plasma emission intensity. The plasma emission intensity plotted in Figure 2a corresponds to the integrated areal intensity after baseline subtraction and fitting these peaks with a Gaussian lineshape. Here, the plasma emission intensity serves as a proxy for the relative plasma density. While we do not have a way to quantify the absolute plasma density, these measurements provide a relative measure of the plasma density. Figure 2b,c shows the raw spectra taken at peak voltages of 4.5 and 5 kV, respectively. All spectra shown here are baseline-subtracted. The data shown in Figure 2 was taken with a constant laser power density of 2.4 W/cm² focused through a cover glass-corrected, high numerical aperture objective lens. As illustrated in Figure 2, it should be noted that plasma can be initiated at a lower pulse voltage threshold (i.e., 4.0 kV) with laser irradiation than is possible without irradiation (i.e., 4.5 kV). However, the enhancement of plasma emission intensity with laser irradiation decreases at higher voltages. In the range of lower applied pulse voltages (i.e., 4-5 kV), the limiting factor for plasma emission is the hot electron population, which can be significantly modified under laser irradiation. However, at high peak voltages (i.e., 5.5 kV), photoexcited hot electrons are not needed in order to initiate the plasma. Here, the limiting factor becomes field emission of electrons from the NPs (and copper electrodes), and thus, laser irradiation has a limited effect on the plasma emission

While Figure 2a shows the peak pulse voltage dependence of plasma emission, Figure 3 shows the laser power dependence of the plasma emission intensity, which shows a linear dependence on the laser power. These data were taken with AuNPs instead of platinum NPs at a fixed pulse peak voltage of 2.4 kV. Here, the plasma is initiated at a much lower peak pulse

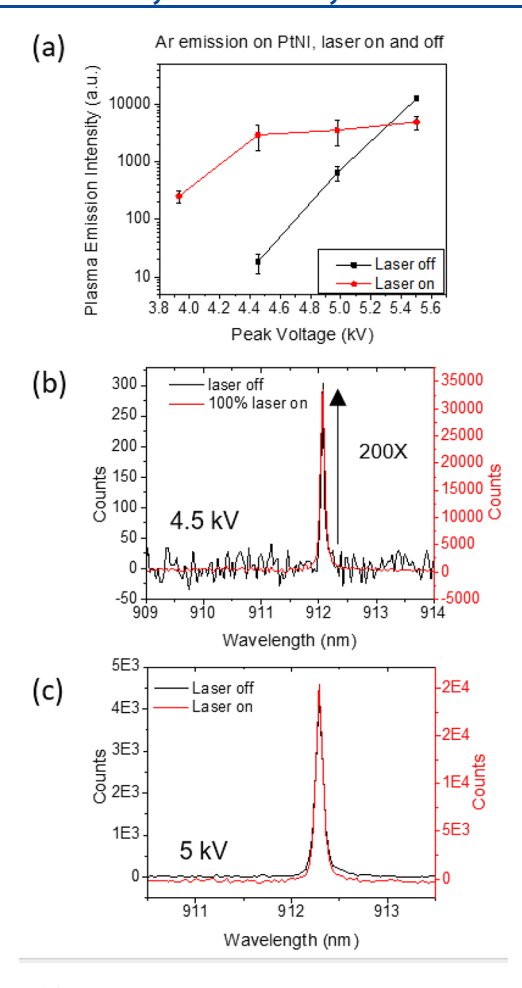


Figure 2. (a) Plasma emission intensity plotted as a function of peak pulse voltage with and without 532 nm laser illumination observed from Pt nanoparticles. Plasma emission spectra under (b) 4.5 and (c) 5 kV peak voltage with and without 532 nm laser illumination on Pt nanoparticles.

voltage of 2.4 kV, likely because of the lower work function of gold compared with platinum and gold's strong interband transitions around 532 nm wavelength (i.e., 2.4 eV) that originate from the d-band electrons in gold.^{37–39} Interestingly, no enhancement in the plasma emission was observed with 633 nm photons (i.e., 1.96 eV) or 785 nm photons (i.e., 1.58 eV) since these photons lie below the threshold for interband transitions in Au. Another possible explanation is the sample-to-sample variation. That is, small variations in the size, shape, and separation of the NPs can lead to large changes in the local fields and, hence, plasma initiation voltage.²⁴ Nevertheless, it should be noted that all quantitative comparisons in plasma emission intensity were done on the same sample. Therefore, this sample-to-sample variation will not affect the main conclusions of this paper.

Figure 4 shows the energy band diagrams illustrating the hot electron-driven process by which plasma emission is enhanced in these metal NP geometries. Figure 4a shows the energy band diagram for a typical metal with no photoexcitation. Here, the work function, which needs to be overcome in order for thermionic emission to occur, thus initiating plasma discharge, is approximately 5.1 eV. Figure 4b illustrates the case with photoexcited hot carriers in the metal, where a photon excites an electron at the Fermi energy to 2.4 eV above the Fermi energy, thus lowering the effective work function by

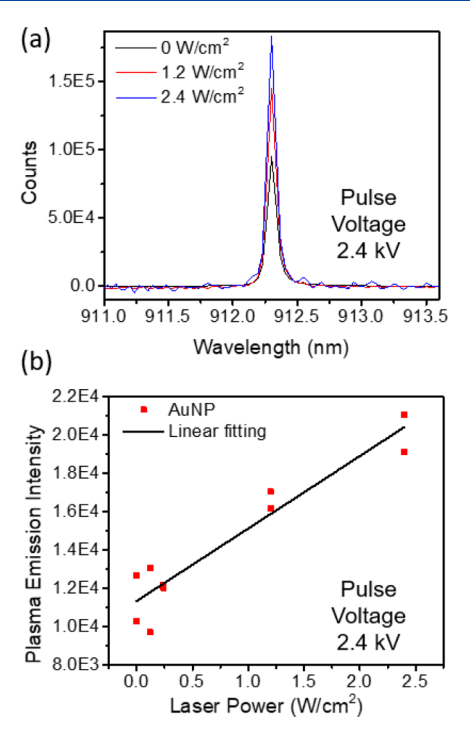


Figure 3. (a) Plasma emission spectra observed from AuNPs under different laser illumination conditions. (b) Plasma emission intensity observed by discharging 2.4 kV pulses across AuNPs plotted as a function of laser power. The laser wavelength here is 532 nm.

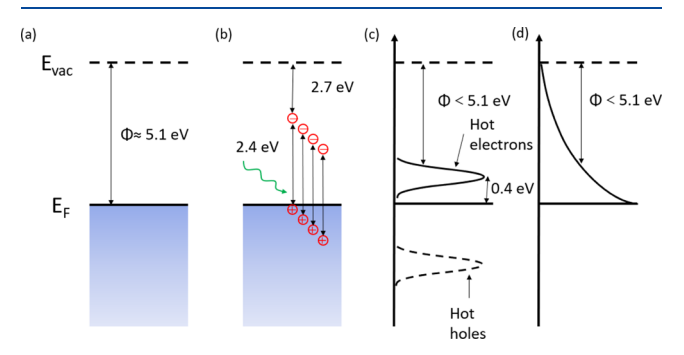


Figure 4. Energy band diagrams of AuNPs (a) without and (b) with 532 nm wavelength laser irradiation. Illustration of hot electron distributions at (c) \sim 50 fs and (d) \sim 2 ps.

as much as 2.4 eV. In gold, there are a large number of states corresponding to d-band electrons, which lie roughly 2 eV below the Fermi level. ^{37,38} As such, the hot electrons that are actually formed by a 2.4 eV photon are centered around an energy of approximately 0.4 eV above the Fermi energy, as illustrated in Figure 4c. This results in a lower effective work function ($\Phi \approx 4.7$ eV). However, it should be noted that the lowering of the effective work function results in an exponential increase in thermionic emission and, hence, plasma discharge intensity. The hot electron distribution illustrated in Figure 4c decays over very short time scales, less than 50 fs. Based on our previous work using ultrafast pumpprobe spectroscopy (i.e., transient absorption spectroscopy), this narrow distribution of hot electrons decays into a hot Fermi distribution, as illustrated in Figure 4d. This hot Fermi distribution decays back to equilibrium with the lattice temperature over a timescale of 2 ps, 40-43 as shown in Figure S3 of the Supporting Information. Here, we believe it is the electrons in the tail of this hot Fermi distribution that contribute most significantly to the effect observed in this paper.

CONCLUSIONS

In conclusion, we demonstrate that transient plasma discharge across metal NPs can be enhanced up to 200× under 532 nm wavelength laser illumination. This enhancement is achieved by laser-induced hot electron excitation, which can generate large hot electron populations and reduce the effective work function of the material, enabling increased electron emission from the metal NP surfaces. Due to the small size of these NPs, which are on the order of the mean free path of the electrons, these hot electrons have a high probability of traveling to the NP surfaces and, thus, being emitted by the applied electric field. No enhancement is observed under 633 nm wavelength illumination, which lies below the threshold for interband transitions in these metals. Because of the exponential dependence of electron field emission and hence plasma initiation, this general scheme provides a sensitive method for studying these relatively short-lived hot electrons. This reported enhancement in plasma generation is induced by photoexcitation and thus opens up a new potential pathway for photon energy utilization and harvesting by assisting plasma generation and potentially driving chemical reactions near the metal NP surface.

ASSOCIATED CONTENT

Supporting Information

The Supporting Information is available free of charge at https://pubs.acs.org/doi/10.1021/acs.jpcc.1c00765.

Experimental setup, plasma emission intensity under 633 and 785 nm laser illumination, and transient absorption spectra revealing photoexcited hot electron lifetime in Au (PDF)

AUTHOR INFORMATION

Corresponding Author

Stephen B. Cronin — Department of Physics and Astronomy, University of Southern California, Los Angeles, California 90089, United States; Ming Hsieh Department of Electrical Engineering and Department of Chemistry, University of Southern California, Los Angeles, California 90089, United States; Occid.org/0000-0001-9153-7687;

Email: scronin@usc.edu

Authors

Bofan Zhao — Ming Hsieh Department of Electrical Engineering, University of Southern California, Los Angeles, California 90089, United States; orcid.org/0000-0003-0478-6330

Indu Aravind – Department of Physics and Astronomy, University of Southern California, Los Angeles, California 90089, United States

Sisi Yang — Department of Physics and Astronomy, University of Southern California, Los Angeles, California 90089, United States; orcid.org/0000-0003-0352-833X

Yu Wang — Mork Family Department of Chemical Engineering and Materials Science, University of Southern California, Los Angeles, California 90089, United States; orcid.org/0000-0002-0307-1301

Ruoxi Li — Mork Family Department of Chemical Engineering and Materials Science, University of Southern California, Los Angeles, California 90089, United States

Boxin Zhang — Mork Family Department of Chemical Engineering and Materials Science, University of Southern California, Los Angeles, California 90089, United States

Yi Wang – Department of Chemistry, University of Southern California, Los Angeles, California 90089, United States

Jahan M. Dawlaty — Department of Chemistry, University of Southern California, Los Angeles, California 90089, United States; orcid.org/0000-0001-5218-847X

Complete contact information is available at: https://pubs.acs.org/10.1021/acs.jpcc.1c00765

Notes

The authors declare no competing financial interest.

ACKNOWLEDGMENTS

This research was supported by the Army Research Office (ARO) award no. W911NF-19-1-0257 (B.Z.) and no. W911NF-17-1-0325 (Y.W.), the National Science Foundation (NSF) award no. CHE-1954834 (R.L.) and CHE-1708581 (I.A.), and Air Force Office of Scientific Research (AFOSR) grant no. FA9550-19-1-0115 (S.Y.).

REFERENCES

- (1) Park, J. Y.; Baker, L. R.; Somorjai, G. A. Role of Hot Electrons and Metal—Oxide Interfaces in Surface Chemistry and Catalytic Reactions. *Chem. Rev.* **2015**, *115*, 2781–2817.
- (2) Diesing, D.; Janssen, H.; Otto, A. Surface reactions with hot electrons and hot holes in metals. Surf. Sci. 1995, 331–333, 289–293.
- (3) Hou, B.; Shen, L.; Shi, H.; Kapadia, R.; Cronin, S. B. Hot electron-driven photocatalytic water splitting. *Phys. Chem. Chem. Phys.* **2017**, *19*, 2877–2881.
- (4) Zhang, Y.; He, S.; Guo, W.; Hu, Y.; Huang, J.; Mulcahy, J. R.; Wei, W. D. Surface-Plasmon-Driven Hot Electron Photochemistry. *Chem. Rev.* **2018**, *118*, 2927–2954.
- (5) Tagliabue, G.; Jermyn, A. S.; Sundararaman, R.; Welch, A. J.; DuChene, J. S.; Pala, R.; Davoyan, A. R.; Narang, P.; Atwater, H. A. Quantifying the role of surface plasmon excitation and hot carrier transport in plasmonic devices. *Nat. Commun.* **2018**, *9*, 3394.
- (6) Rezaeifar, F.; Ahsan, R.; Lin, Q.; Chae, H. U.; Kapadia, R. Hotelectron emission processes in waveguide-integrated graphene. *Nat. Photonics* **2019**, *13*, 843–848.
- (7) Mudi, P.; Khamari, S. K.; Sharma, T. K. Role of Hot Electrons in the Development of GaAs-Based Spin Hall Devices with Low Power Consumption. *Phys. Status Solidi RRL* **2020**, *14*, 2000097.
- (8) Wei, J.; Olaya, D.; Karasik, B. S.; Pereverzev, S. V.; Sergeev, A. V.; Gershenson, M. E. Ultrasensitive hot-electron nanobolometers for terahertz astrophysics. *Nat. Nanotechnol.* **2008**, *3*, 496–500.
- (9) Guo, J.; Zhang, Y.; Shi, L.; Zhu, Y.; Mideksa, M. F.; Hou, K.; Zhao, W.; Wang, D.; Zhao, M.; Zhang, X.; et al. Boosting Hot Electrons in Hetero-superstructures for Plasmon-Enhanced Catalysis. *J. Am. Chem. Soc.* **2017**, *139*, 17964–17972.
- (10) Kang, Y.; Gong, Y.; Hu, Z.; Li, Z.; Qiu, Z.; Zhu, X.; Ajayan, P. M.; Fang, Z. Plasmonic hot electron enhanced MoS 2 photocatalysis in hydrogen evolution. *Nanoscale* **2015**, *7*, 4482–4488.
- (11) Yokoyama, N.; Imamura, K.; Ohshima, T.; Nishi, H.; Muto, S.; Kondo, K.; Hiyamizu, S. Tunneling Hot Electron Transistor Using GaAs/AlGaAs Heterojunctions. *Jpn. J. Appl. Phys., Part* 2 **1984**, 23, L311–L312.
- (12) Levi, A. F. J.; Chiu, T. H. Room-temperature operation of hotelectron transistors. *Appl. Phys. Lett.* **1987**, *51*, 984–986.
- (13) Vaziri, S.; Lupina, G.; Henkel, C.; Smith, A. D.; Ostling, M.; Dabrowski, J.; Lippert, G.; Mehr, W.; Lemme, M. C. A Graphene-Based Hot Electron Transistor. *Nano Lett.* **2013**, *13*, 1435–1439.

- (14) Zeng, C.; Song, E. B.; Wang, M.; Lee, S.; Torres, C. M.; Tang, J.; Weiller, B. H.; Wang, K. L. Vertical Graphene-Base Hot-Electron Transistor. *Nano Lett.* **2013**, *13*, 2370–2375.
- (15) Mooney, J. M.; Silverman, J. The theory of hot-electron photoemission in Schottky-barrier IR detectors. *IEEE Trans. Electron Devices* **1985**, 32, 33–39.
- (16) LaPierre, R. R.; Robson, M.; Azizur-Rahman, K. M.; Kuyanov, P. A review of III—V nanowire infrared photodetectors and sensors. *J. Phys. D: Appl. Phys.* **2017**, *50*, 123001.
- (17) Feng, B.; Zhu, J.; Lu, B.; Liu, F.; Zhou, L.; Chen, Y. Achieving Infrared Detection by All-Si Plasmonic Hot-Electron Detectors with High Detectivity. *ACS Nano* **2019**, *13*, 8433–8441.
- (18) Neugebauer, C. A.; Webb, M. B. Electrical Conduction Mechanism in Ultrathin, Evaporated Metal Films. *J. Appl. Phys.* **1962**, 33, 74–82.
- (19) Dittmer, G. Electrical conduction and electron emission of discontinuous thin films. *Thin Solid Films* **1972**, *9*, 317–328.
- (20) Borziak, P. G.; Kulyupin, Y. A.; Nepijko, S. A.; Shamonya, V. G. Electrical conductivity and electron emission from discontinuous metal films of homogeneous structure. *Thin Solid Films* **1981**, *76*, 359–378
- (21) Borziak, P. G.; Kulyupin, Y. A. Investigations of discontinuous metal films in the U.S.S.R. *Thin Solid Films* **1977**, *44*, 1–19.
- (22) Borziak, P.; Kulyupin, Y.; Tomchuk, P. Electron processes in discontinuous metal films. *Thin Solid Films* **1975**, *30*, 47–53.
- (23) Fedorovich, R. D.; Naumovets, A. G.; Tomchuk, P. M. Electron and light emission from island metal films and generation of hot electrons in nanoparticles. *Phys. Rep.* **2000**, 328, 73–179.
- (24) Zhao, B.; Aravind, I.; Yang, S.; Cai, Z.; Wang, Y.; Li, R.; Subramanian, S.; Ford, P.; Singleton, D. R.; Gundersen, M. A.; et al. Nanoparticle-Enhanced Plasma Discharge Using Nanosecond High-Voltage Pulses. *J. Phys. Chem. C* **2020**, *124*, 7487–7491.
- (25) Zhao, B.; Aravind, I.; Yang, S.; Wang, Y.; Li, R.; Cronin, S. B. Au Nanoparticle Enhancement of Plasma-Driven Methane Conversion into Higher Order Hydrocarbons via Hot Electrons. ACS Appl. Nano Mater. 2020, 3, 12388.
- (26) Aden, M.; Kreutz, E. W.; Voss, A. Laser-induced plasma formation during pulsed laser deposition. *J. Phys. D: Appl. Phys.* **1993**, 26, 1545–1553.
- (27) Aden, M.; Beyer, E.; Herziger, G. Laser-induced vaporisation of metal as a Riemann problem. *J. Phys. D: Appl. Phys.* **1990**, 23, 655–661.
- (28) Vadillo, J. M.; Laserna, J. J. Laser-induced plasma spectrometry: truly a surface analytical tool. *Spectrochim. Acta, Part B* **2004**, 59, 147–161.
- (29) Aragón, C.; Aguilera, J. A. Characterization of laser induced plasmas by optical emission spectroscopy: A review of experiments and methods. *Spectrochim. Acta, Part B* **2008**, *63*, 893–916.
- (30) Willmott, P. R.; Huber, J. R. Pulsed laser vaporization and deposition. *Rev. Mod. Phys.* **2000**, *72*, 315–328.
- (31) Tognoni, E.; Palleschi, V.; Corsi, M.; Cristoforetti, G. Quantitative micro-analysis by laser-induced breakdown spectroscopy: a review of the experimental approaches. *Spectrochim. Acta, Part B* **2002**, *57*, 1115–1130.
- (32) Lowndes, D. H.; Geohegan, D. B.; Puretzky, A. A.; Norton, D. P.; Rouleau, C. M. Synthesis of Novel Thin-Film Materials by Pulsed Laser Deposition. *Science* **1996**, *273*, 898–903.
- (33) Norlén, G. Wavelengths and Energy Levels of Ar I and Ar II based on New Interferometric Measurements in the Region 3 400-9 800 Å. *Phys. Scr.* **1973**, *8*, 249–268.
- (34) Pavaskar, P.; Theiss, J.; Cronin, S. B. Plasmonic hot spots: nanogap enhancement vs. focusing effects from surrounding nanoparticles. *Opt. Express* **2012**, *20*, 14656–14662.
- (35) Qiu, J.; Zeng, G.; Pavaskar, P.; Li, Z.; Cronin, S. B. Plasmonenhanced water splitting on TiO²-passivated GaP photocatalysts. *Phys. Chem. Chem. Phys.* **2014**, *16*, 3115–3121.
- (36) Chien, T.-m.; Pavaskar, P.; Hung, W. H.; Cronin, S.; Chiu, S.-H.; Lai, S.-N. Study of the Plasmon Energy Transfer Processes in Dye Sensitized Solar Cells. *J. Nanomater.* **2015**, 2015, 139243.

- (37) Sundararaman, R.; Narang, P.; Jermyn, A. S.; Goddard, W. A., III; Atwater, H. A. Theoretical predictions for hot-carrier generation from surface plasmon decay. *Nat. Commun.* **2014**, *5*, 5788.
- (38) Brown, A. M.; Sundararaman, R.; Narang, P.; Goddard, W. A.; Atwater, H. A. Nonradiative Plasmon Decay and Hot Carrier Dynamics: Effects of Phonons, Surfaces, and Geometry. *ACS Nano* **2016**, *10*, 957–966.
- (39) Michaelson, H. B. The work function of the elements and its periodicity. *J. Appl. Phys.* **1977**, *48*, 4729–4733.
- (40) Wang, Y.; Shi, H.; Shen, L.; Wang, Y.; Cronin, S. B.; Dawlaty, J. M. Ultrafast Dynamics of Hot Electrons in Nanostructures: Distinguishing the Influence on Interband and Plasmon Resonances. *ACS Photonics* **2019**, *6*, 2295–2302.
- (41) Wang, Y.; Aravind, I.; Cai, Z.; Shen, L.; Gibson, G. N.; Chen, J.; Wang, B.; Shi, H.; Song, B.; Guignon, E.; et al. Hot Electron Driven Photocatalysis on Plasmon-Resonant Grating Nanostructures. *ACS Appl. Mater. Interfaces* **2020**, *12*, 17459–17465.
- (42) Aravind, I.; Wang, Y.; Cai, Z.; Shen, L.; Zhao, B.; Yang, S.; Wang, Y.; Dawlaty, J. M.; Gibson, G. N.; Guignon, E.; et al. Hot Electron Plasmon-Resonant Grating Structures for Enhanced Photochemistry: A Theoretical Study. *Crystals* **2021**, *11*, 118.
- (43) Wang, Y.; Shen, L.; Wang, Y.; Hou, B.; Gibson, G. N.; Poudel, N.; Chen, J.; Shi, H.; Guignon, E.; Cady, N. C.; et al. Hot electron-driven photocatalysis and transient absorption spectroscopy in plasmon resonant grating structures. *Faraday Discuss.* **2019**, 214, 325–339.